Materials Transactions, Vol. 43, No. 5 (2002) pp. 1079 to 1084
Special Issue on Hydrogen Absorbing Materials

Phase Diagram and Superabundant Vacancy Formation in Cr–H Alloys

Yuh Fukai and Masaki Mizutani *

Department of Physics, Chuo University, Tokyo 112-8551, Japan

X-ray diffraction measurements on the Cr–H system were made using synchrotron radiation at high hydrogen pressures and high temperatures, and the phase diagram was determined up to $p(H_2) = 5.5\,GPa$ and $T \lesssim 1400\,K$. Three solid phases were found to exist; a bcc phase (α) of low hydrogen concentrations, $x = [H]/[Cr] \lesssim 0.03$ existing at low hydrogen pressures ($\lesssim 4.4\,GPa$), and two high-pressure phases, an hcp (ε) phase at lower temperatures and an fcc (γ) phase at higher temperatures, both having high hydrogen concentrations $x \sim 1$. A drastic reduction of the melting point is caused by dissolution of hydrogen. A gradual lattice contraction observed in the fcc phase indicates the formation of superabundant Cr-atom vacancies (vacancy-hydrogen clusters). Thermal desorption measurements after recovery from high $p(H_2)$, T treatments revealed several desorption stages including those due to the release from vacancy-hydrogen clusters and from hydrogen-gas bubbles, and allowed determination of relevant trapping energies.

(Received February 25, 2002; Accepted March 8, 2002)

Keywords: *chromium, hydrogen, phase diagram, superabundant vacancy, high pressure, X-ray diffraction*

1. Introduction

Metallic chromium, in its ordinary bcc structure, can dissolve only small amounts of hydrogen, but is known to form hydrides having hcp and fcc structures (ε and γ phases). (For old literatures, see Refs. 1–3).) Both these hydrides were originally formed by cathodic electrodeposition of Cr,[4] but one of them (hcp) was later synthesized by direct reaction with high pressure H_2 gas as well,[5] and the bcc-hcp boundary was determined in the range of H_2 pressure up to $p(H_2) = 1.6\,GPa$ and temperature up to $T \lesssim 700\,K$.[6,7] The structure of the hcp hydride was determined by neutron diffraction to be of NiAs type with Cr atoms occupying the As sites,[8] and its composition was close to $x = [H]/[Cr] = 1.0$. The hydrogen concentration of the fcc hydride appeared to be higher ($x \geq 1.0$), and was initially identified with dihydride of CaF_2 type by analogy with other metal-hydrogen systems,[9] but in fact rather variable depending on the condition of sample preparation. Most recent work of Tkacz[10] showed that the fcc hydride of composition close to $x = 1$ could be prepared by keeping the electrode temperature low (277–283 K). The fcc hydride thus prepared was however reported to be unstable and decompose in time in bursts, in contrast to the hcp hydride which could be stored indefinitely under ambient conditions.[11] The equation of state (the pressure-volume relation) of the fcc and hcp hydrides measured up to 37 GPa was found to be very similar. Only the initial volume was slightly different; $14.38 \times 10^{-3}\,nm^3$ (fcc) vs. $14.16 \times 10^{-3}\,nm^3$ (hcp).[10]

The primary purpose of the present paper was to determine the phase diagram of the Cr–H system over a much wider range of H_2 pressure and temperature by *in situ* X-ray diffraction (XRD) and characterize the structure of the existing phases. The state of hydrogen in these phases was investigated by thermal desorption spectroscopy (TDS) on specimens after recovery from high $p(H_2)$, T treatments. In the course of these experiments, we discovered evidence of superabundant vacancy (SAV) formation, as observed in several other metal-hydrogen alloys,[12–20] and investigated the SAV formation process in some detail.

2. Experimental Methods

The XRD measurements were made using synchrotron radiation at Photon Factory in Tsukuba, where a cubic-anvil press MAX80 specifically designed for high p, T measurements is installed.

A high-purity (99.99%) powder sample of #400-mesh size, mixed with BN powder to reduce excessive absorption of X-rays, was formed into pellets of $\phi 1 \times (0.2–0.3)$ mm, sealed in a capsule of NaCl together with an internal hydrogen source ($NaBH_4 + Ca(OH)_2$) and a pressure marker (NaCl + BN), and was placed at the center of a cubic cell of edge length 8 mm or 10 mm made of a solid pressure-transmitting medium (amorphous B-epoxy resin composite). A nearly homogeneous pressure up to $\sim 7\,GPa$ could be applied to the sample by compressing the cell from six perpendicular directions with WC anvils of top faces $6\,mm \times 6\,mm$. An electric current ($\leq 100\,A$) supplied to a graphite tube heater around the capsule could raise the temperature to ca. 1300 K, and supply H_2 to the sample by the decomposition of the hydrogen source at $\gtrsim 500\,K$. Thin BN plates separated the sample and the hydrogen source, and prevented contamination of the sample. The temperature was measured by a C-A thermocouple placed at the outside wall of the heater, and pressure was determined by measuring the lattice parameter of NaCl using a Decker scale.[21] Details of the sample cell assembly were described elsewhere.[19]

For XRD measurements, the energy-dispersive method was adopted, where diffracted X-rays were energy-analyzed by an SSD placed at a fixed angle ($2\theta \fallingdotseq 6°$) from the incident beam. The beam was collimated to a slice of 0.1 mm to assure high energy resolutions. With these devices an XRD pattern was obtained in 60–100 s, with the accuracy of lattice parameter measurements typically better than 0.1%.

TDS measurements were made on specimens recovered from heat treatments under H_2 pressures of 1.8 and 4.4 GPa, for which a similar cubic-anvil press (Oz-F1) or a small-scale piston-cylinder press was used depending on the required ex-

*Graduate Student, Chuo University.

perimental conditions. A sample was held at a high $p(H_2)$, T condition for a certain duration of time (15 min $\sim$ 5 h), rapidly cooled to room temperature in a few seconds, decompressed, and recovered to ambient conditions. After recovery, a sample was transferred to a thermal-desorption spectrometer, evacuated, and heated at a rate of 5 K/min. In order to examine possible changes of state and loss of hydrogen, TDS measurements were made at various times after recovery from heat treatments.

3. Experimental Results

3.1 Phase diagram

X-ray diffraction measurements were performed under fixed ram loads, at appropriate temperature intervals in the course of heating. At each temperature, a sample was equilibrated for about 5 min before the measurement.

A phase diagram was constructed from a series of such measurements at several different ram loads, with the result shown in Fig. 1. The result agrees reasonably well with the bcc-hcp ($\alpha - \varepsilon$) boundary reported previously in the low $p(H_2)$-T region.[6,7] A striking reduction of the melting point is indicated by a data at $\sim$3 GPa. Similar melting-point reductions by dissolution of hydrogen were observed in other metal-hydrogen systems as well (Ti–H,[22] V–H,[23] Mn–H,[24] Fe–H[25–27]).

3.2 Crystal structure

The temperature dependence of the atomic volume (volume per Cr atom) in the four measuring runs (in Fig. 1) is shown in Fig. 2. Corrections for pressure variation with temperature were not made, but estimated to be reasonably small (Using the bulk modulus of Cr, a pressure variation of 0.5 GPa leads to $\sim$0.3% change in volume). Atomic volumes observed in the hcp (ε) phase at four different pressures are very nearly the same at all corresponding temperatures. The same statement also applies to the bcc (α) and fcc (γ) phases, although the data taken at same temperatures are rather limited to allow detailed comparison. Immediately after quenching and decompression, both the hcp and fcc structures were retained, and the atomic volumes in these states indicated that the H concentrations were retained as well. The stability of these hydrides were, however, very different thereafter. While the hcp hydride remained as such indefinitely under ambient conditions, the fcc hydride decomposed and returned to bcc structure in short times ($\sim$10 min), depending to some extent on the period of heat treatments.

The temperature dependence of the axial ratio in the hcp (ε) phase is shown in Fig. 3. The ratio is nearly constant and close to the ideal ratio $c/a = 1.633$ at all temperatures and pressures.

The temporal variation of the lattice parameter was measured at 1170 K, at two different pressures 2.6 GPa and 5 GPa corresponding to the fcc (γ) and hcp (ε) phases respectively. The results are shown in Fig. 4. It was noticed that the forma-

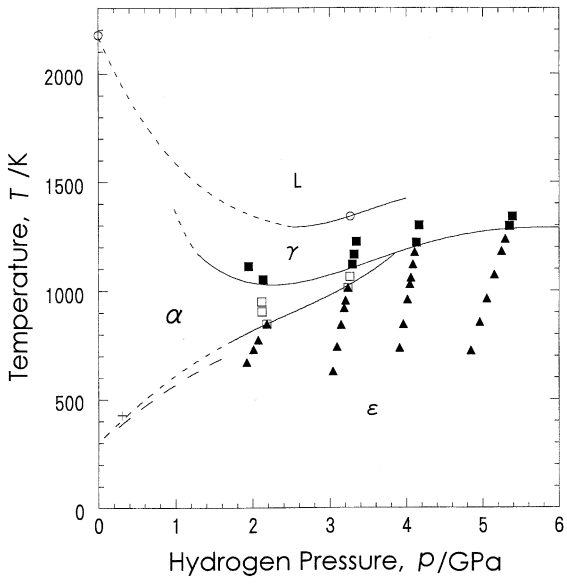

Fig. 1 Phase diagram of the Cr–H system as a function of hydrogen pressure and temperature. The crystal structures are; bcc (α), hcp (ε) and fcc (γ). In the lower p, T region, a cross has been taken from Ref. 6), and a broken line from Ref. 7).

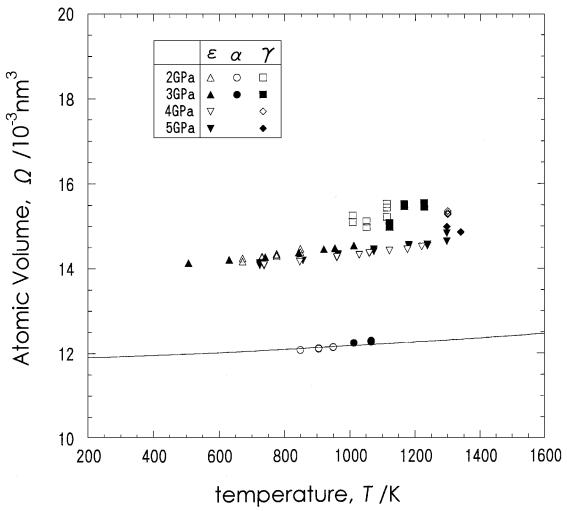

Fig. 2 Temperature dependence of the atomic volume (volume per Cr atom) at four different hydrogen pressures, encompassing three different phases; bcc (α), hcp (ε) and fcc (γ). A curve drawn in the lower part of the Figure represent the thermal expansion of metallic Cr at ambient pressure.[29]

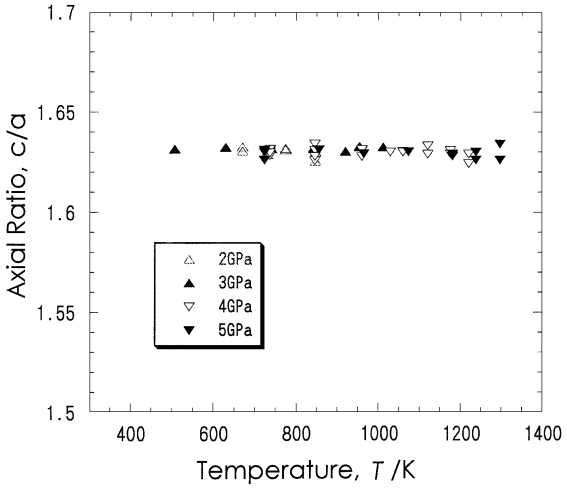

Fig. 3 Temperature dependence of the axial ratio of the hcp phase (ε) at four different hydrogen pressures.

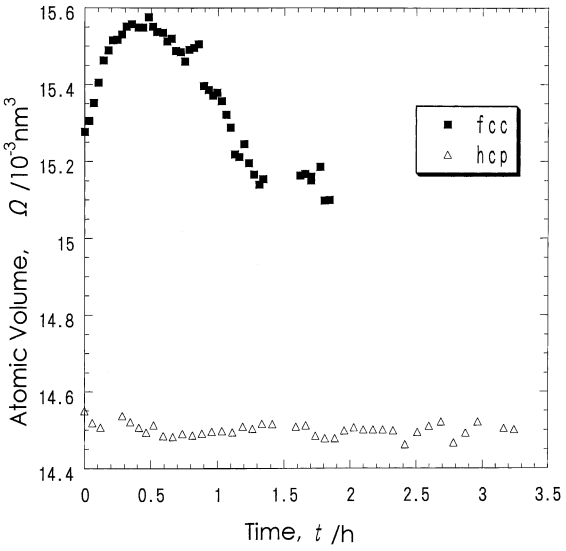

Fig. 4 Atomic volume (volume per Cr atom) of fcc (γ) and hcp (ε) hydride as a function of holding time at 1170 K, $p(H_2) = 2.6$ GPa and 5 GPa, respectively.

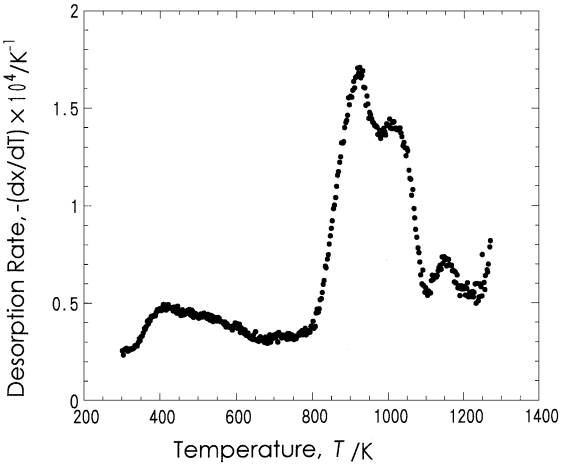

Fig. 5 A thermal desorption spectrum observed after quenching from the bcc (α) phase. The heat treatment was made at 1.8 GPa, 870 K for 3 h. Measurements were made at 20 min after recovery to ambient condition.

tion (and decomposition) of the fcc (γ) phase was rather slow; the initial volume increase should imply that the equilibium hydrogen concentration was reached after $\sim$20 min. No such delays were observed in the formation/decomposition of the hcp (ε) phase. The subsequent lattice contraction observed in the fcc (γ) phase indicative of SAV formation will be discussed later.

3.3 Thermal desorption

A typical thermal desorption spectrum observed after quenching from the bcc (α) phase is shown in Fig. 5. The heat treatment was made at 1.8 GPa and 870 K for 3 h, and the measurement was made at 20 min after recovery. There is a broad peak at high temperatures, extending over 900–1200 K, and the amount of desorbed hydrogenin this stage is $x \approx 0.033$.

After quenching from the hcp (ε) phase, desorption spectra became very simple, as shown in Fig. 6. The spectrum measured 33 min after recovery from 4.4 GPa, 1070 K for

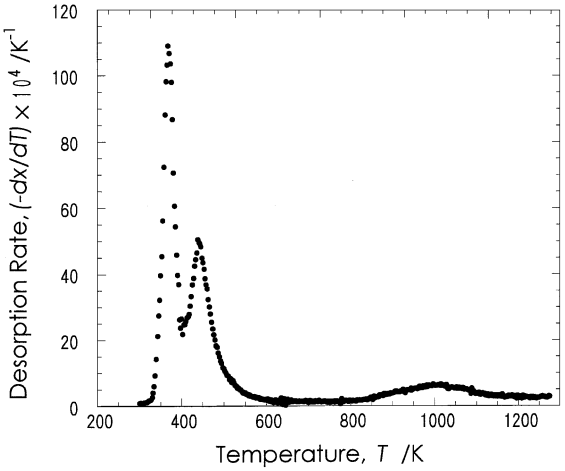

Fig. 6 A thermal desorption spectrum observed after quenching from the hcp (ε) phase. The heat treatment was made at 4.4 GPa, 1070 K for 15 min, and the measurement was made 33 min after recovery.

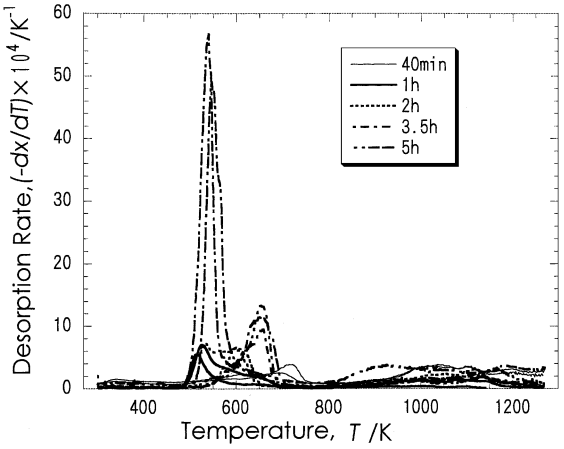

Fig. 7 Thermal desorption spectra observed after heat treatments in the fcc (γ) phase. The heat treatments were performed at 1.8 GPa, 1170 K for 40 min, 1 h, 2 h, 3.5 h and 5 h. The measurements were made at various times after recovery.

15 min consists of two major peaks; a sharp pronounced peak at 370 K and a broad peak at 430 K. A closer inspection reveals a broad peak centered around $\sim$1000 K. The amount of hydrogen desorbed in these three stages are $x = 0.38$, 0.35 and 0.19 in the order of increasing temperature, giving a total of $x = 0.92$. The structure changed from hcp to bcc after degassing at 370 K.

Thermal desorption spectra after heat treatments in the fcc (γ) phase (1.8 GPa, 1170 K) changed with holding time, as shown in Fig. 7. The desorption took place between 450 K and 750 K, roughly in three stages centered around 540 ± 20 K, 660 ± 10 K and 710 ± 20 K, and the total amount of desorbed hydrogen in these stages increased with increasing holding time. The measurements were made at different times after recovery, and their spectral shape was rather variable, but the peak temperatures were fairly well defined. In all these measurements, a broad additional peak of hydrogen content $x \approx 0.06$ was observed at high temperatures. XRD data showed that a small amount of fcc phase became stable under ambient conditions after long heat treatments, the existing ratio of fcc to bcc phases being $\sim 1 : 10$ after 2 h holding and $\sim 3 : 4$ after 5 h holding. The structure returned to bcc

after the two major desorption stages were completed.

4. Discussion

4.1 Structure and composition of different phases

One of the peculiar features of the Cr–H system is that, a Cr metal, which occurs only in the bcc structure at all pressures and temperatures, can easily be transformed into an hcp structure at reasonably low hydrogen pressures. This is because the formation energy of hcp hydride (25 kJ/mol H[6]) is much lower than the heat of solution in the bcc phase (58 kJ/mol H[28]).

In Fig. 2, the bcc data points lie closely on the thermal expansion curve of metallic Cr at ambient pressure,[29] which indicates that H concentrations are negligibly small under these $p(H_2)$-T conditions. The solubility calculated by using the heat of solution of 58 kJ/mol H is $x \approx 0.01$–0.03 between 900–1200 K at 3 GPa,[30] which is consistent with this observation. The concentration observed in the recovered specimen ($x \approx 0.033$) is also consistent with these values. For the hcp (ε) phase, all the data points in Fig. 2 lie fairly well on a single straight line, with a slope almost parallel to the bcc data, the difference between the hcp and bcc data being $(2.6 \pm 0.1) \times 10^{-3}\,\mathrm{nm}^3$. This indicates that hydrogen concentrations of the hcp phase were nearly the same, probably close to the stoichiometric limit $x = 1.0$. Previous reports have also shown that hcp hydrides prepared by electrodeposition have compositions always close to $x = 1.0$. As the reference volume of the hcp structure should be smaller than that of the bcc structure by $0.1 \times 10^{-3}\,\mathrm{nm}^3$ (*e.g.* in Fe, the difference being $0.13 \times 10^{-3}\,\mathrm{nm}^3$ for bcc $\rightarrow$ fcc ($\alpha \rightarrow \gamma$) transition, and $0.07 \times 10^{-3}\,\mathrm{nm}^3$ for fcc $\rightarrow$ bcc ($\gamma \rightarrow \delta$)[31]), the volume per H atom in the hcp phase can be estimated at $\Omega_H = (2.7 \pm 0.2) \times 10^{-3}\,\mathrm{nm}^3$. This value is consistent with the general trend of H-induced volumes in transition metals.[32,33] The TDS data indicates that 10% of hydrogen was lost in the recovery process.

Figure 2 shows that the atomic volume of fcc (γ) hydrides is $(15.0$– $15.6) \times 10^{-3}\,\mathrm{nm}^3$, which is larger than that of bcc Cr by $(2.7$–$3.3) \times 10^{-3}\,\mathrm{nm}^3$. Assuming a reference volume of (hypothetical) fcc Cr to be smaller than bcc Cr by $\sim 0.1 \times 10^{-3}\,\mathrm{nm}^3$, we obtain the H-induced volume of $(2.8$–$3.4) \times 10^{-3}\,\mathrm{nm}^3$. Values of this magnitude may be assigned to monohydride.

4.2 Interpretation of thermal desorption spectra

The spectrum observed after recovery from the hcp (ε) phase (Fig. 6) serves as a clue for unravelling the implications of all the other results. There, the major peak (located at 373 ± 2 K, the average of 3 runs) should be due to the desorption of H atoms through the hcp lattice.

The desorption temperature of H atoms on regular interstitial sites in the bcc lattice can be estimated by comparing the migration energies in hcp and bcc lattices. The migration energy of H atoms in the hcp lattice can be estimated to be $e_m(\mathrm{hcp}) \approx 51$ kJ/mol by interpolation of experimental values on two 3d metals in the hcp phase; 52 kJ/mol for Ti and 50 kJ/mol for Co,[34] whereas the value for the bcc lattice to be $e_m(\mathrm{bcc}) = 4.1$ kJ/mol by interpolation of 4.3 kJ/mol for V and 3.9 kJ/mol for Fe.[33] If we assume that a proportionality relation holds between the migration energy and desorption peak temperature, we can estimate the desorption temperature of H atoms on regular interstitial sites in the bcc lattice; $T_p \approx 373 \times 4.1/51 = 30$ K. This implies that most H atoms should be desorbed immediately after quenching from the bcc phase; all the remaining H atoms should therefore be in some trapped states. This statement applies to all the desorption peaks observed in the present experiment excepting the two major peaks in the hcp phase.

The assignment of these other desorption peaks is rather straightforward. The broad high-temperature peak, which appears in all the cases, should be due to desorption from voids formed by precipitation of supersaturated hydrogen. From the activation energy roughly estimated to be $51 \times 1000/373 = 137$ kJ/mol, the binding energy can be obtained by subtracting the migation energy, *i.e.* $e_b \approx 133$ kJ/mol. The value compares reasonably well with the estimate for voids; the difference of the chemisorption energy and the heat of solution gives 138 kJ/mol.[35]

The two pronounced peaks which appeared after heat treatments in the fcc (γ) phase can be identified as detrapping from Vac-H clusters. Vac-H clusters created in the fcc phase should be retained in the bcc lattice, and release H atoms in the course of TDS measurements. From the activation energies $e_{a1} = 51 \times (540 \pm 20)/373 = 74 \pm 3$ kJ/mol and $e_{a2} = 51 \times (660 \pm 10)/373 = 90 \pm 1$ kJ/mol, the binding energies can be obtained as $e_{b1} = 70 \pm 3$ kJ/mol and $e_{b2} = 86 \pm 1$ kJ/mol. More detailed discussions on Vac-H clusters will be made in the next sub-section. A small subsidiary peak at ~ 710 K, which disappeared at longer holding times, may probably be due to detrapping from some pre-existing traps.

4.3 Formation of superabundant vacancies

The temporal variation of the atomic volume during the heat treatments (Fig. 4) indicates that a large number of Vac-H clusters (SAVs) were formed in the fcc (γ) phase. This contraction process in the fcc phase appears very similar to the processes observed in other fcc M-H alloys.[12–15,19,20] The observed kinetics and the magnitude of lattice contraction suggest that Vac-H clusters of ~ 10 at% were created at the surface and diffused into the interior of the particles. The observed lattice contraction $\Delta\Omega/\Omega = -0.026$ divided by the relaxation volume of $v_{cl}^R/\Omega = -0.3$[37] gives the cluster concentration $x_{cl} = 0.09$.

The amount of hydrogen desorbed after heat treatments in the fcc phase (Fig. 7) is shown in Fig. 8, as a function of holding time. The observed increase of the retained hydrogen content is similar to the lattice contraction process. Detrapping from Vac-H clusters in two stages separated by ~ 100 K is in fact a common trend in many M-H alloys, and has been attributed to different binding energies for low and high occupancies.[38,39] In the case of Cr, previous measurements of D-implantation and annealing[35] led to an approximate estimate of the binding energy of ~ 80 kJ/mol for Vac-H clusters of the lowest occupancy ($\sim 1:1$).[40] This value agrees well with the binding energy estimated for the 660 K peak. The difference of the binding energies of 540 K and 660 K peaks is also comparable to those reported for several other M-H

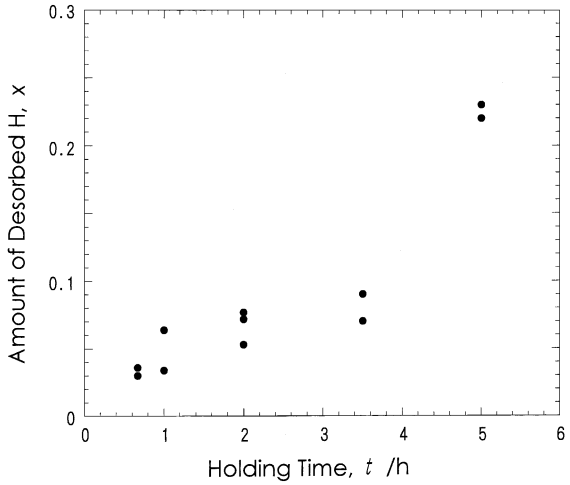

Fig. 8 The amount of hydrogen desorbed after heat treatments in the fcc phase (1.8 GPa, 1170 K) for variable lengths of time. The amounts desorbed between 450 K and 750 K have been included.

alloys.[39)]

The small lattice contraction in the hcp phase appears to indicate that the number of Vac-H clusters was appreciably smaller. A similar dependence on the crystal structure was noticed in the Mn-H system where the lattice contraction was observed conspicuously in the fcc phase, whereas it was scarcely visible in the dhcp phase.[19)] More detailed studies are needed to clarify the origin of this apparent structure dependence.

Lastly, a possible implication of SAV formation for the electrodeposition process will be mentioned. Quite unlike our observation of the slow vacancy formation at high temperatures, which is rate-limited by solid-state diffusion, the stable structure could be reached directly in electrodeposition because hydrogen and metal atoms are deposited simultaneously. The process is like laying bricks for building a designed structure. We have encountered a similar process of SAV formation in Pd-Rh alloys, where the lattice-contracted phase (a defect structure) appeared instantly after melting and re-solidification, whereas it took more than several hours to form the defect structure by solid state diffusion.[41)] This possible facility of defect formation in the electrodeposition process was in fact suggested by Roy and Gibb in as early as 1967,[11)] but has been largely forgotten since.

5. Summary and Conclusions

By *in situ* X-ray diffraction at high hydrogen pressures and temperatures and thermal desorption measurements of recovered specimens, it has been shown that monohydrides of Cr having hcp and fcc structures can be formed by direct reaction with molecular hydrogen, in addition to a dilute solid solution in a bcc phase. A $p(H_2)$-T phase diagram consisting of these three phases has thus been constructed in the range $p(H_2) \lesssim 5.5$ GPa and $T \lesssim 1400$ K. By combination of the *in situ* XRD and TDS on recovered samples, evidence has been obtained for the formation of superabundant vacancies of Cr atoms (Vac-H clusters) in the fcc phase, with concentrations amounting to ~ 10 at%.

Acknowledgments

This work has been supported in part by a Grant-in-Aid for Scientific Research on Priority Areas A of "New Protium Function" from the Ministry of Education, Science, Sports and Culture. The experiments at Photon Factory were performed under Approval 00G027. We wish to thank T. Kikegawa of KEK for his general support, and many members of our laboratory for their help in the experiment.

REFERENCES

1) K. M. Mackey: *Hydrogen Compounds of the Metallic Elements*, (E. & F. Spon, London, 1966).
2) B. Siegel and G. G. Libowitz: *Metal Hydrides*, Ed. by W. M. Mueller, J. P. Blackledge and G. G. Libowitz (Academic Press, New York, 1968) pp. 546–674.
3) B. Baranowski: *Hydrogen in Metals II*, Ed. by G. Alefeld and J. Völkl (Springer, Heidelberg, 1978) pp. 157–200.
4) C. A. Snavely: Trans. Electrochem. Soc. **92** (1947) 537–577.
5) B. Baranowski and K. Bojarski: Roczn. Chem. **46** (1972) 525–527.
6) B. Baranowski, K. Bojarski and M. Tkacz: *Proc. IV Intern. Conf. on High Pressure, Kyoto, 1974*, (The Physico-Chemical Soc. Japan, Kyoto, 1975) pp. 577–579.
7) E. G. Ponyatovsky and I. T. Belash: Dokl. Akad. Nauk SSSR **229** (1976) 1171.
8) G. Albrecht, D. Doenitz, K. Kleinstuck and M. Betal: Phys. Status Solidi **3** (1963) K249.
9) C. A. Snavely and D. A. Vaughan: J. Am. Chem. Soc. **71** (1949) 313–314.
10) M.Tkacz: Polish J. Chem. **71** (1997) 1735–1741.
11) R. J. Roy and T. R. P. Gibb: Jr. J. Inorg. Nucl. Chem. **29** (1967) 341–345.
12) Y. Fukai and N. Ōkuma: Jpn. J. Appl. Phys. **32** (1993) L1256–1259.
13) Y. Fukai and N. Ōkuma: Phys. Rev. Lett. **73** (1994) 1640–1643.
14) Y. Fukai, Y. Ishii, Y. Goto and K. Watanabe: J. Alloys. Compd. **313** (2000) 121–132.
15) Y. Fukai, Y. Kurokawa and H. Hiraoka: J. Japan Inst. Metals **61** (1997) 663–670.
16) H. Ōsono, T. Kino, Y. Kurokawa and Y. Fukai: J. Alloys. Compd. **231** (1995) 41–45.
17) Y. Fukai: *Computer Aided Innovation of New Materials II*, Ed. by M. Doyama, J. Kihara, M. Tanaka and R. Yamamoto (Elsevier, 1993) pp. 451–456.
18) M. Iwamoto and Y. Fukai: Trans. JIM **40** (1999) 606–611.
19) Y. Fukai, T. Haraguchi, E. Hayashi, Y. Ishii, Y. Kurokawa and J. Yanagawa: Defect Diffusion Forum **194** (2001) 1063–1068.
20) Y. Fukai, Y. Shizuku and Y. Kurokawa: J. Alloys. Compd. **329** (2001) 195–201.
21) D. L. Decker: J. Appl. Phys. **36** (1965) 157–159.
22) K. Nakamura and Y. Fukai: J. Alloys. Compd. **231** (1995) 46–50.
23) Y. Fukai, K. Nakamura, Y. Endo and N. Ōkuma: *Proc. Advanced Materials '93, V/B: Shape Memory Materials and Hydrides*, Ed. by K. Otsuka and Y. Fukai (Elsevier, Amsterdam, 1994) pp. 1291–1294.
24) Y. Fukai, T. Haraguchi, H. Shinomiya and K. Mori: Script Mater., In press.
25) T. Suzuki, S. Akimoto and Y. Fukai: Phys. Earth Planet. Inter. **36** (1984) 135–144.
26) T. Yagi and T. Hishinuma: Geophys. Res. Lett. **22** (1995) 1933–1936.
27) T. Okuchi: J. Phys.: Condens. Matter **10** (1998) 11595–11598.
28) E. Fromm and G. Hörz: Intern. Metals Rev. **25** (1980) 269–311.
29) Y. S. Touloukian, R. K. Kirby, R. E. Taylor and P. D. Desai: *Thermophysical Properties of Matter*, Vol. 12, (IFI/Plenum, New York, 1975) p. 61.
30) H. Sugimoto and Y. Fukai: Acta Metall. **40** (1992) 2327–2336.
31) W. B. Pearson: *A Handbook of Lattice Spacings and Structures of Metals and Alloys*, (Pergamon Press, London, 1958).
32) H. Peisl: *Hydrogen in Metals I*, Ed. by G. Alefeld and J. Völkl, (Springer, Heidelberg, 1978) pp. 53–74.
33) Y. Fukai: *The Metal Hydrogen System*, (Springer, Berlin, 1993) Chapter 3.2.
34) J. Völkl and G. Alefeld: *Diffusion in Solids Recent Development*, Ed. by A. S. Nowick and J. J. Burton (Academic Press, New York, 1975)

pp. 231–302.
35) P. Nordlander, J. K. Nørskov and F. Besenbacher: J. Phys. F: Met. Phys. **16** (1986) 1161–1171.
36) J. P. Hirth: Metall. Trans. **11A** (1980) 861–890.
37) P. A. Korzhavyi, I. A. Abrikosov, B. Johansson, A. V. Ruban and H. L. Skriver: Phys. Rev. B **59** (1999-II) 11693–11703.
38) P. Nordlander, J. K. Nørskov, F. Besenbacher and S. M. Myers: Phys. Rev. B **40** (1989-II) 1990–1992.
39) Y. Fukai: *The Metal Hydrogen System*, (Springer, Berlin, 1993) Chapter 4.5.
40) S. T. Picraux: Nucl. Instrum. Methods **182/183** (1981) 413–437.
41) K. Watanabe, N. Okuma, Y. Fukai, Y. Sakamoto and Y. Hayashi: Scr. Mater. **34** (1996) 551–557.